Vol. 02, Iss. 2 (2025) 72-82, DOI: 10.61552/JSI.2025.02.003

Journal of Sustainable Development Innovations

www.jsi.aspur.rs

Computational Investigation of Cs_2BiAgI_6 for Perovskite Solar Cell Applications Using SCAPS-1D

Md Shawon[a], Md Al Araf[a], Supto Kumar Ghosh[a], S.K. Neamul Hasan[a], Utsa Sen[a]

[a]*Bangladesh University of Business and Technology (BUBT), Dhaka, Bangladesh*

Keywords:

Lead free double perovskite material (Cs2BiAgI6), Perovskite solar cells (PSC), SCAPS-1D Simulation, Power conversion efficiency (PCE), Band gap engineering, Thermal stability.

* Corresponding author:

Md Al Araf
E-mail: md.al.araf.2001@gmail.com

Received: 14 August 2024
Revised: 24 September 2024
Accepted: 19 October 2024

A B S T R A C T

This work studies the possibility of Cs_2BiAgI_6, a lead-free double perovskite material, as a light absorber in PSCs. Different device designs were simulated using SCAPS software to optimize power conversion efficiency across varied temperatures, absorber thicknesses and bandgaps. The influence of HTLs and ETLs on device performance was further explored. Among the simulated structures, Str. 1 (TCO/TiO_2/Cs_2BiAgI_6/Cu_2O/Ag) attained the maximum PCE of 22.2% at a thickness of 700 nm, highlighting the importance of adjusting absorber layer thickness for efficiency enhancement. The investigation demonstrated a tradeoff between bandgap and electrical properties, where a larger bandgap led to lower Jsc but a greater Voc. Str. 2 (TCO/ZnO/Cs_2BiAgI_6/Cu_2O/Ag) displayed the highest PCE of 20.72% at 300 K with a 1.7 eV bandgap and a 500 nm thick absorber layer. However, increasing temperature to 380 K resulted in a considerable fall in open circuit voltage (Voc) and PCE for all configurations, illustrating the thermal sensitivity of these devices. Str. 3 (TCO/SnO_2/Cs_2BiAgI_6/CBTS/Au) displayed the greatest PCE of 21% with a 1.45 eV bandgap, underscoring the necessity of bandgap engineering in PSC design. The research studied the JV characteristics and Quantum Efficiency of the simulated devices. Str. 1 demonstrated an extraordinary broad- spectrum absorption of around 97% at 360 nm, showing its potential for efficient light harvesting across a wide range of the solar spectrum. These findings show that Cs_2BiAgI_6 based PSCs have promise as highly efficient and stable replacements to traditional solar cells also the path for the development of sustainable and cost-effective solar energy conversion devices based on lead free double perovskites.

1. INTRODUCTION

Perovskite solar cells (PSCs) are emerging as frontrunners in the race for next-generation photovoltaic technology [1]. With a PCE exceeding 25.2%, they surpass established competitors like CIGS (copper indium gallium selenide) and CdTe (cadmium telluride) [2]. Perovskite materials excel in solar cells due to their unique properties: high ion mobility, long-

lived charge carriers (lasting microseconds) and extended diffusion lengths (hundreds of nanometers). These traits enable efficient charge transport within the device and reduced excitation binding energy, ultimately leading to superior solar cell operation. However, PCE in PSCs is not static. It depends heavily on the composition and design of individual cell layers. Parameters like open-circuit voltage (Voc), fill factor (FF) and short-circuit current (Jsc) all contribute to the overall PCE and each can be optimized through strategic device design. Notably, the perovskite crystal structure allows for precise control over the materials band gap, which in turn influences light absorption, performance and stability [3]. For instance, a band gap of 1.6 eV is considered ideal for capturing a significant portion of the solar spectrum while maintaining a good voltage output. This control over the band gap, achieved through the perovskite crystal structure, highlights a key advantage of the material. Beyond structural modifications, researchers are actively exploring improved synthesis techniques to further elevate PSC performance [4, 5]. To enhance perovskite solar cell performance, researchers are actively developing improved perovskite materials through compositional, defect and crystal growth engineering. Additionally, the choice of electron and hole transport layers is crucial, as these layers significantly impact efficiency by directing charge carriers. Copper oxide and spiro-OmeTAD are common hole transport materials, while titanium dioxide and tin dioxide are widely used for electron transport [6]. PSCs have emerged as a revolutionary photovoltaic technology due to their potential for exceeding the efficiency of traditional silicon cells. However, unlocking their full potential necessitates a comprehensive understanding physical phenomena governing their operation. This includes intricacies like charge transport, recombination (the detrimental process where generated current is lost), and ion migration within the perovskite and transport layers can significantly impact performance. Research efforts are actively directed towards elucidating these processes to optimize device functionality and achieve superior solar energy conversion [7]. This chapter goes into the development of perovskite for third generation solar cells. It studies material alternations, fabrication procedures, device obstacles and stability issues. Additionally, it addresses fundamental physics topics governing PSC functions, such as exciton production, point defects, ion migration, ferroelectric characteristics, charge transport and recombination. By understanding these characteristics and through continued research, we may further improve PSC technology and unlock its full potential as a clean and efficient energy source, with the potential for achieving higher efficiencies in the near future.

2. LITERATURE REVIEW

The chapter discusses studies by Das et al. who studied the possibilities of lead free CsGeI3 PSCs using SCAPS-1D modelling. Their investigation produced a promising power conversion efficiency (PCE) of 19.30% for a device with a precisely tailored absorber layer thickness of 1.4 μm [8]. Pavu et al. identified two key factors for optimizing tandem perovskite/silicon solar cells: a perovskite layer thickness of 300 nm and the presence of p-type doping within the perovskite absorber layer. Their research suggests that these elements are critical for achieving the highest possible PCE in such devices [9]. Sharma et al. investigated the optimization of light absorption efficiency in planar PSCs. Their approach involved strategically manipulating the thickness of the electron and hole transport layers within the device architecture [10]. According to Sharma et al.'s simulation study, a low bandgap PSC design incorporating a mixed Tin (50%) and Lead (50%) halide perovskite material achieved a noteworthy power conversion efficiency of 19.21% [11]. Hu et al. presented a critical review of bandgap engineering strategies for perovskite solar cells. Their analysis focused on two main approaches: impurity doping and pressure application, detailing the mechanism behind each. Additionally, the review explored less established techniques like introducing intermediate bands and using external electric fields for bandgap manipulation. The work concluded by outlining promising future research directions in this field [12]. Kim et al. offered a complete analysis spanning the fundamental optoelectronic features of perovskite materials, with crucial methodologies for constructing high-performance PSCs. They further studied potential next generation solutions for overcoming the Shockley Queisser limit and generating even larger PCEs. [13]. Wu et al. announced a

breakthrough in lead free PSCs by demonstrating the first device utilizing a Cs2AgBiBr6 double perovskite layer. This new cell attained a PCE of 1.44%, displaying promise for environmentally friendly perovskite photovoltaics with good stability under ambient circumstances. Notably the fabrication procedure adopted for this device was relatively straightforward, employing low-pressure aided solution processing [14].

3. METHODOLOGY

The replication and study of the perovskite architecture have been undertaken using the SCAPS-1D program, a solar cell capacitance simulator. This sophisticated tool allows for the modification of numerous solar cell layouts to boost their efficiency dramatically. During the simulation of solar cell layouts, SCAPS-1D carries out calculations based in the Poisson equation as well as the continuity equations for electrons and holes individually. By exploiting these fundamentals equations, the software delivers vital insights into the behavior and performance of perovskite solar cells, paving the door for further breakthroughs in photovoltaic technology.

3.1 Equations of Continuity Poisson's Equation

Do not use further subdivision, for instance 2.1.1. is not allowed. In the absence of light or recombination events, the concentration of free electronics must remain uniform throughout a solar cell device in steady state conditions, consistent with the principle of charge conservation this principal similarity applies to free holes within the device. In solar cell devices, where both generation and recombination processes occur, the conservation of free electrons and holes is governed by continuity equations,

$$\frac{\partial n}{\partial t} = -\frac{\partial J_n}{\partial x} + G - \Re_n \quad (1)$$

$$\frac{\partial p}{\partial t} = -\frac{\partial J_p}{\partial x} + G - \Re_p \quad (2)$$

Where, Gs are light rates of production and ℜs were recombination rates within the device. Poisson's equation delineates the electric field (E) modulation arising from the current flow and charges distributed across the decentralized states, traps, and recombination centers within the device,

$$\frac{\partial}{\partial x}\left(\varepsilon \frac{\partial \Psi}{\partial x}\right) = -q\left[p - n + N_D^+ - N_A^- + \frac{\rho_{def}}{q}\right] \quad (3)\ [1]$$

The equation provided illustrates the connection between electrostatic potential (ψ), dielectric constant (ε), and electronic charge (q) in a given system. Within this framework, the symbol ψ signifies the electrostatic potential present, ε stands for the dielectric constant, and q represents the electronic charge within the system. The equation itself is composed of four distinct terms displayed on the right-hand side, with the first two terms specifically relating to the volume density of free charge carriers. Following these, the subsequent pair of terms are indicative of ionized donor and acceptor-like dopants, which signify localized states within the system. Moreover, the term "def." is used to indicate the presence of defect charge density within the system, adding another layer of complexity to the equation and its implications.

3.2 Equation describing transport

The mobility of free electrons and holes, along with fluctuations in carrier concentration and the resultant variations in quasi-Fermi level, contribute to the generation of electron and hole current. Thus, in a state of thermal equilibrium,

$$J_n = -\frac{\mu_n n}{q}\frac{\partial E_{Fn}}{\partial x} \quad (4)$$

$$J_p = +\frac{\mu_p p}{q}\frac{\partial E_{Fp}}{\partial x} \quad (5)$$

when the parameters μ_n and μ_m indicate the mobility of electronics and holes respectively and n and p express the density of free electronics and holes, the symbols E_{Fn} and E_{Fp} are used to signify the quasi Fermi levels of electrons and holes respectively in the given context [1, 2].

SCAPS-1D has been applied in the examination of various performance metrics of perovskite solar cells, including fill factor, short circuit current density, open circuit voltage and power conversion efficiency. Researchers have employed SCAPS-1D to model numerous configurations of double halide like CS_2TiI_6 perovskite solar cells containing titanium. These simulations explore different combinations of hole transport layers – HTLs and electron transport layers – ETLs to optimize cell performance. The typical perovskite solar cell structure features an absorber layer sandwiched between the ETL and HTL. This creates a basic layout like: TCO/ETL/perovskite/HTL/Metal contact. Studies have investigated and evaluated a wide variety of cell designs using various three specific perovskite solar cell configurations:

Structure-1: TCO/TiO_2/Cs_2BiAgI_6/Cu_2O/Ag
Structure-2: TCO/ZnO/Cs_2BiAgI_6/CBTS/Ag
Structure-3: TCO/SnO_2/Cs_2BiAgI_6/CBTS/Au

The investigation and explanation of these constructs have been carried out by examining a range of performance indicators, including fill factor, short circuit current density, open circuit voltage and efficiency within the domain of inorganic perovskite solar cells. This methodology allows for a full improvement in the performance of such cell technology.

Table 1. Properties for inorganic perovskite solar cell construction for modelling.

Parameters	TCO	TiO_2	ZnO	SnO_2	Cs_2BiAgI_6	Cu_2O	CBTS
Thickness (nm)	500	35	50	100	600	150	100
Bandgap (eV)	3.5	3.2	3.5	3.6	1.6	2.17	1.9
Electron affinity (eV)	4	4.2	3.9	4	3.9	3.2	3.6
Dielectric Permittivity	9	10	9	9	6.5	7.1	5.4
CB effective Density (1/Cm^3)	2.20E+18	2.20E+18	1E+19	2.20E+18	1E+19	2.50E+18	2.20E+18
VB effective density (1/Cm^3)	1.80E+19	1.80E+19	1E+19	1.80E+19	1E+19	1.80E+19	1.80E+19
Electron Mobility (cm^2 /VS)	20	100	50	100	2	200	30
Hole Mobility (cm^2 /VS)	10	25	2	25	2	80	10
Acceptor Density (1/Cm^3)	1E+15	0	0	0	1E+15	9.1E+21	1.80E+18
Donor Density (1/Cm^3)	1E+21	1E+19	7.10E+19	1E+17	1E+15	0	0

3.3 SCAPS 1D simulation for perovskite absorber layers $CsBiAgI_6$

Simulation research applying SCAPS-1D software have studied the optimization of Cs_2BiAgI_6 by adjusting characteristics such as the thickness of the absorber layer, doping density and defect density, alongside those of the ETL and HTL, modifications can be made to optimize the performance of PSCs. Different materials have been studied for ETLS including TiO_2, ZnO and SnO_2 and HTLs. Through this exploration, PCE have been attained within the range of 21.72% to 23.71%. Furthermore, experiments on $Cs_2AgBiBr_6$ based double PSC have indicated the considerable impact of conduction band offset and absorber film thickness on PCE. Additionally, experiments with Cs_2BiAgI_6 based double perovskite solar cells combining alternate hole-transporting layers like CuSCN, spiro-OmeTAD and an electron transport layer like AZnO have generated a PCE of roughly 24%. The research of a novel $Cs_2AuBiCI_6$ absorber material and simulation of an ITO/TiO_2/Cs_2BiAgI_6/Cu_2O/Ag solar cell structure have showed encouraging findings.

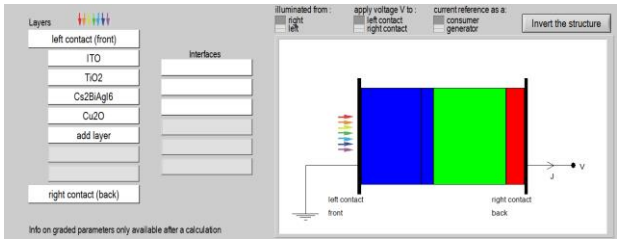

Fig. 1. Structure 1 for TCO/TiO_2/Cs_2BiAgI_6 /Cu_2O/Ag

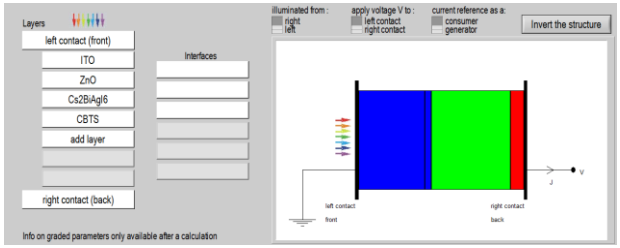

Fig. 2. Structure 2 for TCO/ZnO/Cs_2BiAgI_6/CBTS/Ag

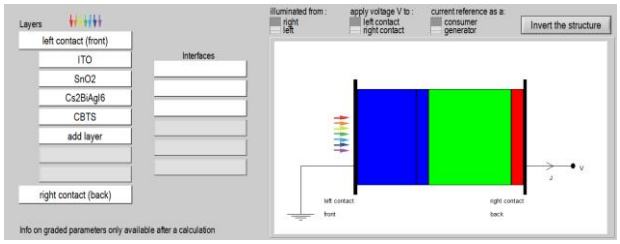

Fig. 3. Stricture 2 for TCO/SnO_2/Cs_2BiAgI_6/CBTS/Au

4. RESULTS AND DISCUSSION

4.1 SCAPS 1D simulation for perovskite absorber layers CsBiAgI6

The overall performance of perovskite solar cells is strongly reliant on the operating temperature, which in this particular example has been altered from 300 K to 380 K. It has been discovered that the efficiency of these solar cells declines as the temperature increases, with the best efficiency being attained at 300 K. Also, several ETL such as TiO_2, ZnO and SnO_2 have been examined, along with diverse HTL including Cu_2O and CBTS as depicted in figure 4 in addition to temperature, other crucial factors like fill factor, open circuit voltage and short circuit potential have also been changed to explore their impact on the overall performance of the solar cells. The link between the short circuit current and the open circuit voltage with respect to temperature fluctuation is clarified. These findings shed light on the delicate interplay between temperature, material choices for ETL and HTL and several other parameters in affecting the efficiency of perovskite solar cells.

$$V_{OC} = \frac{nKT}{q} \log\left(\frac{J_{SC}}{J_o} + 1\right) \quad (6)$$

In this context, Voc is a symbol expressing the Open Circuit Voltage of a system, whilst the parameter n is applied to denote the ideality factor which describes the behavior of the system under investigation. The mathematical expression contains numerous key physical variables such as the Boltzmann constant (k) and the electronic charge (q), which play significant roles in defining the system's behavior. The equation also takes into consideration additional crucial parameters like the Jsc and J_o which are vital for a thorough understanding of the system's properties.

The greatest efficiency observed for structure 1 sits at 22.2%, characterized by an Voc of 0.9797 V, a Jsc of 28.071422 mA/cm^2 and a fill factor of 80.75%. Conversely structure 2, 3 achieved maximum efficiencies of 20.72% and 21.33%, respectively. This data is summarized in the table provided.

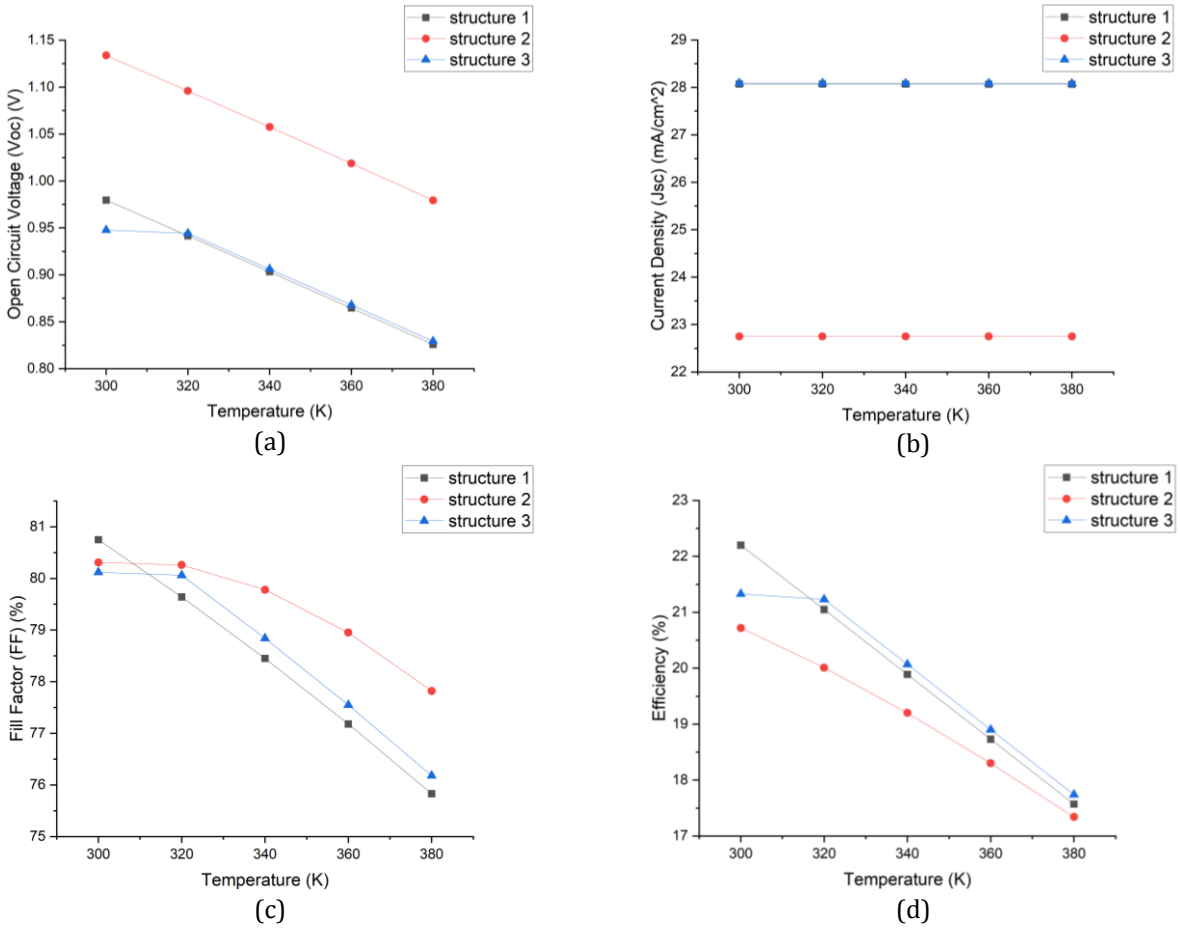

Fig. 4. Variation of performance parameters with temperature, (a) Temp vs Open circuit voltage (b) Temp vs Current density (c) temp vs Fill factor (d) the Efficiency for structure 1, structure 2 and structure 3.

Table 2. Performance metrics of inorganic perovskite solar cells are simulated across varied temperature conditions for three distinct architectures; structure 1, 2 and 3.

Structures	Open Circuit Voltage (V_{OC})(V)	Current Density (J_{SC}) (mA/cm^2)	Fill Factor (%)	Efficiency (%)	Temperature (K)
Structure 1: TCO/TiO_2/Cs_2BiAgI_6 /Cu_2O/Ag	0.9796	28.071422	80.75	22.2	300
	0.9415	28.070462	79.64	21.05	320
	0.9032	28.0689	78.45	19.89	340
	0.8646	28.067089	77.18	18.73	360
	0.8258	28.065411	75.83	17.57	380
Structure 2: TCO/ZnO/Cs_2BiAgI_6 /CBTS/Ag	1.1338	22.75023	80.31	20.72	300
	1.0959	22.749637	80.26	20.01	320
	1.0576	22.749207	79.78	19.2	340
	1.0187	22.748921	78.95	18.3	360
	0.9794	22.749327	77.82	17.34	380
Structure 3: TCO/SnO_2/Cs_2BiAgI_6 /CBTS/Au	0.9478	28.087274	80.12	21.33	300
	0.9441	28.087261	80.06	21.23	320
	0.9062	28.08524	78.84	20.07	340
	0.8679	28.082956	77.55	18.9	360
	0.8293	28.08029	76.18	17.74	380

Moreover, in Figure 4 (a), it can be observed that despite an increase in temperature from 300 K to 380 K, there is a notable decrease in the open-circuit voltage in the simulation results for all structures. Our result shows a voltage decrease, suggesting a decline in both conversion efficiency and fill factor for all structures. Consequently structure 1 appears to outperform structure 2 and 3 at 300 K. This suggests that further research and development on structure 1 might be more promising at this temperature. Interestingly, Jsc remains constant across all structures despite the temperature increase. This implies that current density may not significantly affect the overall performance of the perovskite models with varying HTLs. However, at a higher temperature of 380 K, all simulated structures exhibit a substantial efficiency drop.

4.2 Effect of the thickness of the absorber layer

It is commonly understood that the performance of the device is substantially influenced by the thickness of the absorber layer, a well-documented fact in the field. As the absorber layer thickness increases, there is a general enhancement in light absorption, which is a key parameter for the efficiency of the device. Nevertheless, the presence of thicker absorber layers may introduce unexpected issues such as recombination, attributed to the larger diffusion lengths associated with them. This recombination phenomenon can have a detrimental effect on the power conversion efficiency of the device. Thicker absorber layers can trap more photons, resulting in a higher concentration of carrier charges and consequently, a greater generation of electron-hole pairs. Consequently, this elevated carrier concentration contributes to an increase in the J_{SC} while causing a simultaneous reduction in the V_{OC}, as visually represented in Figure 5 (a) and Figure 5 (b). In the present investigation, a range of absorber layer thicknesses, varying from 300 nm to 700 nm, was explored across a variety of device structures to assess the influence of thickness on different performance parameters.

Thicker absorber layers can lead to a lower fill factor within the structure. This is primarily due to an increase in shunt resistance, which allows unwanted current pathways and reduces the device's ability to convert light into usable electricity. Consequently, a lower fill factor can significantly impact the overall power conversion efficiency of the solar cell. Alterations in light absorption and carrier transportation due to the variation in absorber layer thickness can further complicate the efficiency of the device, making it crucial to carefully consider this parameter during the design and optimization process.

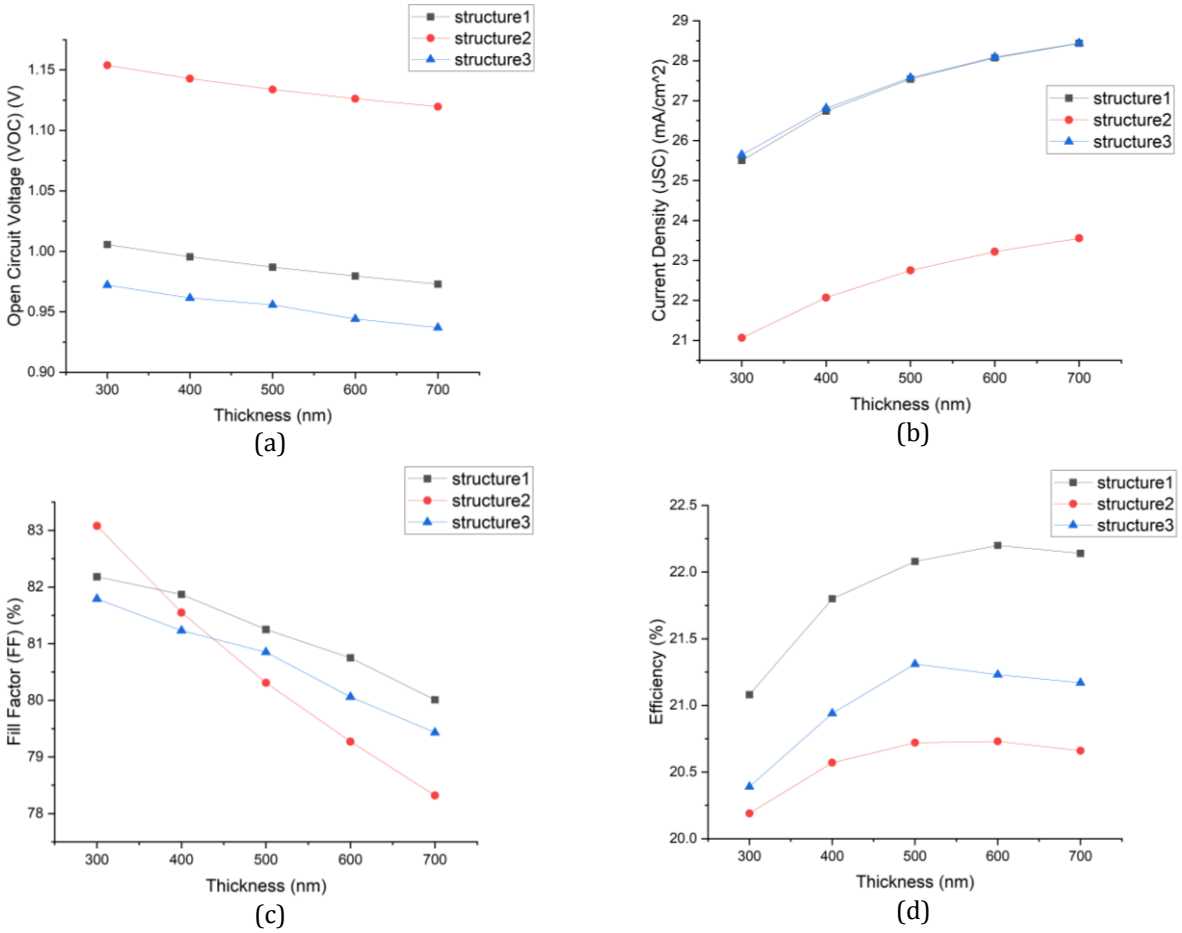

Figure 5: Variation of performance parameters with thickness (a) open circuit voltage (Voc) (b) Jsc current density (c) fill factor (d) the efficiency for structure 1, 2 and 3.

Table 3. Thickness dependence of performance metrics in PSCs.

Structure	Open Circuit Voltage (V_{OC})(V)	Current Density (J_{SC})(mA/cm²)	Fill Factor (%)	Efficiency (%)	Thickness (nm)
Structure 1: TCO/TiO_2/Cs_2BiAgI_6 /Cu_2O/Ag	1.0057	25.502756	82.18	21.08	300
	0.9955	26.741037	81.87	21.8	400
	0.9869	27.538838	81.25	22.08	500
	0.9796	28.071422	80.75	22.2	600
	0.9729	28.437723	80.01	22.14	700
Structure 2: TCO/ZnO/Cs_2BiAgI_6 /CBTS/Ag	1.1538	21.062903	83.08	20.19	300
	1.1429	22.071771	81.55	20.57	400
	1.1338	22.75023	80.31	20.72	500
	1.1262	23.220693	79.27	20.73	600
	1.1197	23.555701	78.32	20.66	700
Structure 3: TCO/SnO_2/Cs_2BiAgI_6 /CBTS/Au	0.9721	25.644949	81.79	20.39	300
	0.9614	26.81131	81.23	20.94	400
	0.9558	27.57339	80.85	21.31	500
	0.9441	28.087261	80.06	21.23	600
	0.937	28.442853	79.43	21.17	700

Based on the simulation findings presented in Figure 5 where structure 1 and 3 exhibit the highest PCE of 22.2%, 21.23% respectively, at a thickness of 600 nm and 500nm. Conversely, Structure 2 achieves a maximum PCE of 20.73% at the same thickness. While the increase in thickness has a minimal effect on Structures 1 and 3, it notably impacts Structure 2. This suggests that while a thicker absorber layer (300–700 nm) increases light absorption, the possibility of sudden recombination in thicker layers can reduce overall PCE. Consequently, it's evident that a thickness of 700 nm yields the highest PCE for Structure 4 compared to Structures 2 and 3. The Table 3 and Figure 5 show a trade-off with increasing absorber thickness: Jsc increases, while Voc decreases.

4.3 Effect of the band gap of the absorber layer

To optimize the photovoltaic effect, it is advisable to provide the absorber layer with 1.6 eV, known as the Shockley-Queisser limit. A suitable power conversion efficiency (PCE) can be attained through precise alignment of band gaps among the absorber layer, HTL, and ETL. The band gap of these materials can be adjusted between 1.45 eV and 1.85 eV on titanium-based perovskites. As depicted in Figure 6 (b), the short circuit current density diminishes due to increased band gap of the absorber layer leading to reduced photon absorption. Moreover, the open circuit voltage rises with an increased band gap, as shown in Figure 6 (a). The rise in volatile organic compounds (V_{OC}) values can be linked to exciton dissociation of charge carriers. The open circuit voltage is influenced by the band gap, resulting in a higher voltage over current. Figure 6 (c) demonstrates that the Fill Factor (FF) peaks at a band gap of 1.6 eV for structure 1. This observation is evident. Nonetheless, the (FF) for structure 3 is observed to decrease, despite minimal differences between structure 1 and structure 2.

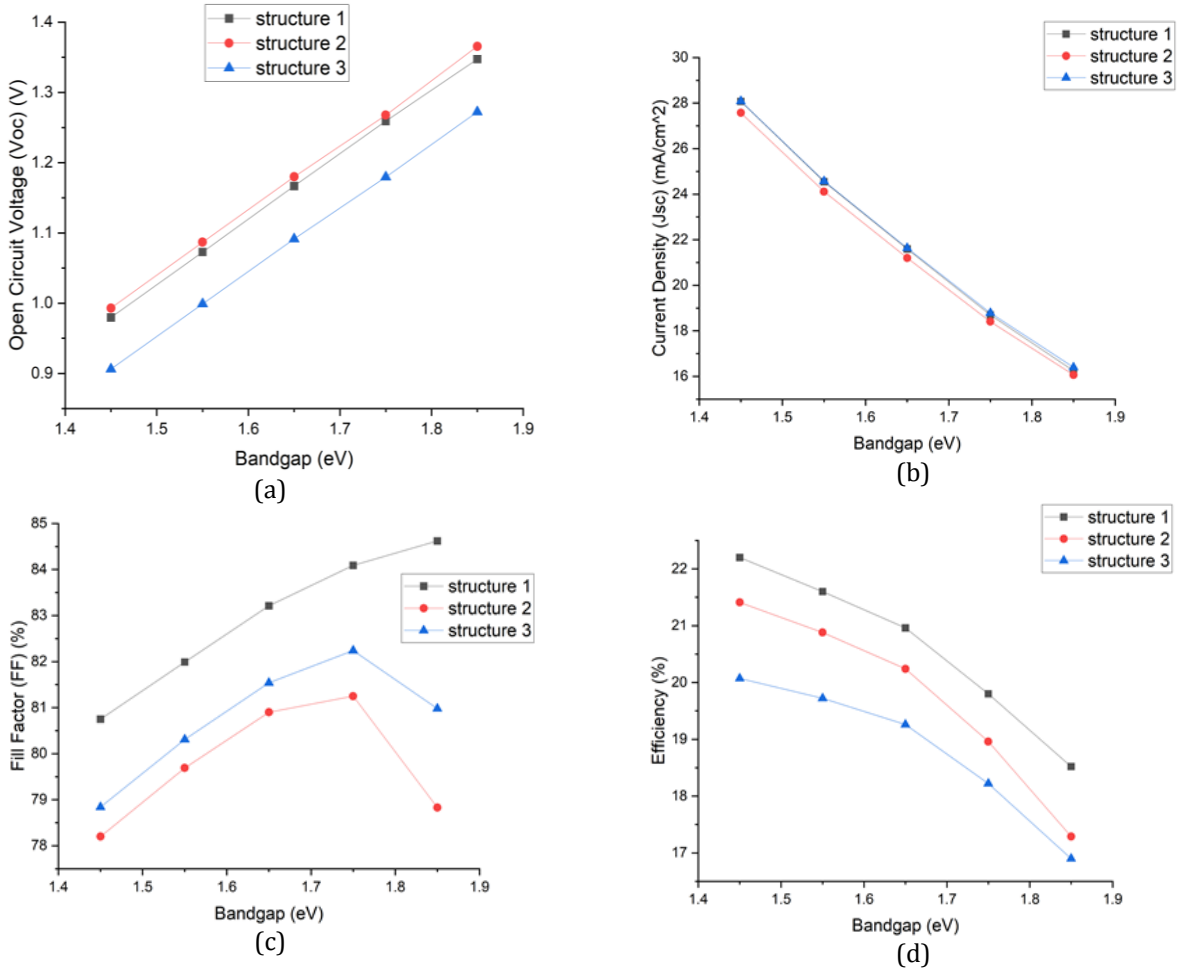

Figure 6. Variation of performance parameters with bandgap (a) open circuit voltage (b) Jsc, current density (c) fill factor (d) the efficiency for structure 1-3.

Table 4. Band Gap dependence of PSC performance for structure 1,2 and 3.

Structure	Open Circuit Voltage (V_{OC})(V)	Current Density (J_{SC}) (mA/cm^2)	Fill Factor (%)	Efficiency (%)	Band-gap (ev)
Structure 1: TCO/TiO_2/Cs_2BiAgI_6 /Cu_2O/Ag	0.9796	28.071422	80.75	22.2	1.45
	1.0729	24.547684	81.99	21.6	1.55
	1.1667	21.589948	83.21	20.96	1.65
	1.2591	18.697486	84.09	19.8	1.75
	1.3474	16.24325	84.62	18.52	1.85
Structure 2: TCO/ZnO/Cs_2BiAgI_6 /CBTS/Ag	0.9931	27.573118	78.2	21.41	1.45
	1.0868	24.111753	79.69	20.88	1.55
	1.1799	21.200327	80.9	20.24	1.65
	1.2677	18.404576	81.25	18.96	1.75
	1.3656	16.063441	78.83	17.29	1.85
Structure 3: TCO/SnO_2/Cs_2BiAgI_6 /CBTS/Au	0.9062	28.08524	78.84	20.07	1.45
	0.9991	24.575271	80.31	19.72	1.55
	1.0915	21.638016	81.54	19.26	1.65
	1.1796	18.780829	82.24	18.22	1.75
	1.2724	16.399329	80.98	16.9	1.85

According to the results obtained from the simulation, it has been determined that Structure 1 demonstrates the highest level of efficiency, amounting to 22.2%, while possessing a band gap of 1.45 eV. The mentioned structure showcases an open-circuit voltage (V_{OC}) of 0.9796 V, a short-circuit current density (J_{SC}) measuring at 28.071422 mA/cm^2, and a fill factor (FF) reaching 80.75%. Conversely, structure 2 and 3 achieve efficiencies about 21.41%, 20.07% respectively, also operating where the band gap of 1.45 eV. It is important to note that these specified levels of efficiency are observed when the thickness is 700 nm and the temperature is set at 300 K, as clearly illustrated in Table 4, which succinctly presents the comparative data for the structures under scrutiny.

4.4 Study of the (J-V) behaviors and QE is conducted in this research

Understanding short circuit current density and voltage behavior is crucial for accurate solar cell modelling. In order to go deeper into these crucial factors, graphical representations of voltage plotted against current density were generated specifically for the BiAg-based perovskite solar cell, as illustrated in Figure 7 (a). The quantum efficiency (QE) curve, displayed in Figure 7 (b), exhibits variations corresponding to different wavelengths within the context of this particular simulation. The Cs2BiAgI6 material showcases a narrow band gap, resulting in an absorption range that extends up to 800 nm for the BiAg-based perovskite solar cell that is structure 1. The quantum efficiency QE curve spans the entire color spectrum from 300 to 700 nm, demonstrating an outstanding broad-spectrum absorption efficiency of approximately 97% at a specific wavelength of 360 nm. This phenomenon indicates an enhanced absorption of photons within the cross-sectional region, as elucidated in Figure 7 (b). The results of the simulation highlight that Structure 1 attains a superior power conversion efficiency (PCE) reaching 22.2%, characterized by an open-circuit voltage (V_{OC}) of 0.9796 V, a short-circuit current density (J_{SC}) of 28.071422 mA/cm^2, and a fill factor (FF) of 80.75%. An exploration was conducted on the influence of temperature variations on both Voc and Jsc, along with an analysis of the correlation between current-density and open circuit voltage, spanning across diverse temperature intervals from 300 K to 380 K, as depicted in Figure 7.

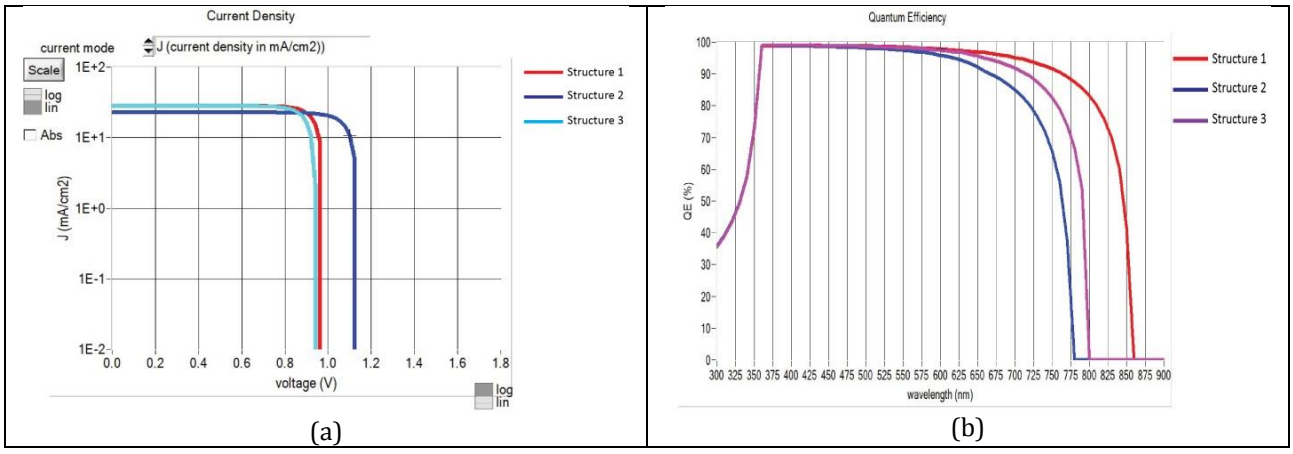

Figure 7. (a) Curve depicting the variation of J-V characteristics and (b) Graph illustrating the relationship between quantum efficiency and wavelength.

5. CONCLUSION

The efficiency of solar cells is substantially influenced by the absorber layer, which is a crucial component. Although augmenting its thickness often enhances light absorption, there is a compromise. Increased thickness of layers can result in elevated recombination rates as a consequence of longer distances traveled by carriers, eventually leading to a reduction in power conversion efficiency (PCE). Investigating absorber thickness from 300 -700 nm and band gap in various solar cell designs, this study found a 700 nm layer maximized efficiency is 22.2% in the Cs_2BiAgI_6 structure. This emphasizes the balancing act between light absorption and recombination for optimal performance. Mentionable is that the thicker layers had minimal impact on specific structures, suggesting their designs effectively address recombination. Beyond thickness, the study highlights the band gaps importance. Optimal performance aligned with Shockley-Queisser limit that is around 1.6 eV. Titanium based perovskites from that is tunable from 1.45 eV – 1.85 eV supports this concept, with structure 7 ($TCO/TiO_2/Cs_2BiAgI_6/Cu_2O/Ag$) achieving the best efficiency of 22.2% at 1.45 eV. This demonstrates well-matched band alignment for efficient excitation separation. Finally, the study emphasizes analyzing short circuit current density and Voc in solar cell models. These along with the quantum efficiency curve, offer valuable insights into light absorption and overall device performance. The simulated BiAg based PSC exemplifies this, achieving a high PCE of 22.2% due to board visible light absorption.

REFERENCES

[1] K. Fatema, "Optimizing inorganic double halide (Cs2TiI6) perovskite solar cell for different hole transport layers using solar cell capacitance software (SCAPS-ID)," *Mater. Today Commun.*, vol. 35, p. 105860, Jun. 2023, doi: 10.1016/j.mtcomm.2023.105860.

[2] K. Fatema and M. S. Arefin, "Enhancing the efficiency of Pb-based and Sn-based perovskite solar cell by applying different ETL and HTL using SCAPS-ID," *Opt. Mater.*, vol. 125, p. 112036, Mar. 2022, doi: 10.1016/j.optmat.2022.112036.

[3] K. Fatema, M. T. Ahmed, Md. K. Hossain, and F. Ahmed, "Structural and Morphological Properties of Single and Mixed Halide Pb-Based Perovskites," *Adv. Condens. Matter Phys.*, vol. 2022, pp. 1–7, Oct. 2022, doi: 10.1155/2022/6001569.

[4] C. S. SOLANKI, *Solar Photovoltaics: Fundamentals, Technologies And Applications*. PHI Learning Pvt. Ltd., 2015.

[5] C. Cho *et al.*, "Multi-bandgap Solar Energy Conversion via Combination of Microalgal Photosynthesis and Spectrally Selective Photovoltaic Cell," *Sci. Rep.*, vol. 9, no. 1, p. 18999, Dec. 2019, doi: 10.1038/s41598-019-55358-6.

[6] J. Tsiba Matondo, D. Malouangou Maurice, Q. Chen, L. Bai, and M. Guli, "Inorganic copper-based hole transport materials for perovskite photovoltaics: Challenges in normally structured cells, advances in photovoltaic performance and device stability," *Sol. Energy Mater. Sol. Cells*, vol. 224, p. 111011, Jun. 2021, doi: 10.1016/j.solmat.2021.111011.

[7] M. Atowar Rahman, "Performance analysis of WSe2-based bifacial solar cells with different electron transport and hole transport materials by SCAPS-1D," *Heliyon*, vol. 8, no. 6, p. e09800, Jun. 2022, doi: 10.1016/j.heliyon.2022.e09800.

[8] A. Das, D. P. Samajdar, and B. Kumar Ravidas, "Investigation of the Efficiency of $CsGeI_3$ -based solar cell using SCAPS-1D modeling and simulation," in *2022 IEEE International Conference of Electron Devices Society Kolkata Chapter (EDKCON)*, Kolkata, India: IEEE, Nov. 2022, pp. 91–95. doi: 10.1109/EDKCON56221.2022.10032870.

[9] K. S. Pavu and J. Jacob, "Evaluation of Performance Parameters of 2T Perovskite/Si Tandem Solar Cells," in *2022 IEEE 19th India Council International Conference (INDICON)*, Kochi, India: IEEE, Nov. 2022, pp. 1–6. doi: 10.1109/INDICON56171.2022.10039757.

[10] V. Sharma, S. Saini, and R. Padmanabhan, "Optimization of Transport Layer Thickness for Perovskite Solar Cells: An Optical Analysis," in *2020 5th IEEE International Conference on Emerging Electronics (ICEE)*, New Delhi, India: IEEE, Nov. 2020, pp. 1–4. doi: 10.1109/ICEE50728.2020.9777084.

[11] S. Sharma, R. Pandey, J. Madan, and R. Sharma, "Optimization of Mixed Sn and Pb Perovskite Solar Cell in Terms of Transport Layers and Absorber Layer Thickness Variation," in *2021 Devices for Integrated Circuit (DevIC)*, Kalyani, India: IEEE, May 2021, pp. 633–636. doi: 10.1109/DevIC50843.2021.9455886.

[12] Z. Hu, Z. Lin, J. Su, J. Zhang, J. Chang, and Y. Hao, "A Review on Energy Band-Gap Engineering for Perovskite Photovoltaics," *Sol. RRL*, vol. 3, no. 12, p. 1900304, Dec. 2019, doi: 10.1002/solr.201900304.

[13] J. Y. Kim, J.-W. Lee, H. S. Jung, H. Shin, and N.-G. Park, "High-Efficiency Perovskite Solar Cells," *Chem. Rev.*, vol. 120, no. 15, pp. 7867–7918, Aug. 2020, doi: 10.1021/acs.chemrev.0c00107.

[14] C. Wu *et al.*, "The Dawn of Lead-Free Perovskite Solar Cell: Highly Stable Double Perovskite $Cs_2AgBiBr_6$ Film," *Adv. Sci.*, vol. 5, no. 3, p. 1700759, Mar. 2018, doi: 10.1002/advs.201700759.